Comparative Genomics and Directed Evolution Reveal Genetic Determinants of Extreme UVC Radiation Tolerance in Bacteria Recovered from the Stratosphere

Adam J. Ellington[a], Tyler J. Schult[a], Christopher R. Reisch[a*], and Brent C. Christner[a#],

[a]Department of Microbiology and Cell Science, Institute of Food and Agricultural Science, University of Florida, Gainesville, Florida, USA

#Address correspondence to Brent C. Christner, xner@ufl.edu.

*Present address: Christopher R. Reisch, Genomatica, San Diego, California, USA

Abstract – 381 words

Main Text – 5610 words

Abstract

Aerosolized microbes surviving transport to and in the stratosphere endure extremes of low temperature, atmospheric pressure, and relative humidity, and high shortwave ultraviolet radiation flux. However, the genetic determinants for traits enabling resistance to the combination of stresses experienced by microbes in the high atmosphere have not been systematically investigated. In this study, we examined Proteobacteria and Actinobacteria isolated from the stratosphere (18 to 29 km ASL) and that demonstrated high tolerance to desiccation (15-25% RH) and UVC radiation (UVCR; λ= 254 nm). Closely related reference strains were more sensitive to UVCR than the stratospheric isolates, indicating that extreme resistance is not universally distributed in these phylogenetically related bacteria. Comparative genomic analyses revealed DNA repair and antioxidant defense genes in the isolates that are not possessed by the related reference strains, including genes encoding photolyase, DNA nucleases and helicases, and catalases. Directed evolution by repeated exposure to increasing doses of UVCR improved the LD_{90} in a sensitive reference strain by ~3.5-fold. The mutations acquired in *Curtobacterium flaccumfaciens pv. flaccumfaciens* strain DSM 20129 incrementally increased its UVCR resistance, with the accumulation of 20 point mutations in protein coding genes increasing tolerance to a level approaching that of stratospheric isolate *Curtobacterium* sp. L6-1. The genetic basis for the increased UVCR tolerance phenotypes observed is discussed, with a specific emphasis on the role of genes involved in DNA repair and detoxification of reactive oxygen species.

Importance

Ultraviolet radiation is omnipresent in sunlight and has important biological effects on organisms. The stratosphere is the only location on Earth where microbes receive natural

exposure to highly mutagenic wavelengths (<280 nm) of ultraviolet radiation. Genetic studies of bacteria from an environment that selects for extreme ultraviolet radiation resistant phenotypes has expanded what is known from studies of model species (e.g., *E. coli*) and identified potentially novel protection and repair strategies. In addition to deepening understanding of ultraviolet radiation photobiology in atmospheric microbes and bacteria in general, these advancements are also highly relevant to astrobiology and space biology. The cold, dry, hypobaric, and high radiation environment of the stratosphere provides an earthly analog for thin extraterrestrial atmospheres (e.g., Mars) and is ideal for bioprospecting extremophile phenotypes that enable engineering of genetic stability and functionality in bio-based space life-support systems or any application where long-term persistence is desirable (e.g., biocontrol).

Introduction

The persistence of microbes during atmospheric transport and deposition has important implications to human health (1, 2), agriculture (3–5), meteorology (6–8), and astrobiology (9, 10). Many studies have focused on microbial aerosols in the lowest layer of the troposphere, where the air is in contact with and affected by the surface (i.e., convective boundary layer, CBL). However, the composition of microbial assemblages in the CBL can be quite different from that of overlying air masses in the 'free troposphere' (11, 12). Importantly, environmental conditions in the CBL are unrepresentative of those at higher altitudes, where biological stresses (e.g., water loss and ultraviolet radiation, UVR) become increasingly intense. Given that 10^{23} to 10^{24} microbes are estimated to disperse annually in the Earth-atmosphere system (13), new information is needed to determine the genetic basis and mechanisms enabling survival under the extreme conditions associated with atmospheric transport.

The stratosphere is the atmospheric layer above the troposphere (~15 to 50 km above sea level, ASL) and is characterized by low temperature, atmospheric pressure, and relative humidity (RH) and high UVR flux (9, 12–16). This combination of conditions is unique to any other location on Earth and similar to conditions on the surface of Mars (14, 15), making the stratosphere a relevant astrobiological analog to examine microbial survival potential on alien worlds (16–19). Microbes that survive conditions in the stratosphere are limited to those tolerant of water loss and exposure to high levels of UVR (20). The UVR spectrum consists of three types: UVAR (320-400 nm), UVBR (280-320 nm), and UVCR (100-280 nm). Oxygen and ozone in the lower stratosphere strongly absorb short wavelength UVR, and consequently, UVCR is not observed at lower altitudes in the troposphere (21). As such, the stratosphere is the

only natural laboratory on Earth to examine the biological effects of high energy UVR wavelengths.

UVR damages cells via direct and indirect effects. Direct absorption of UVR by DNA forms pyrimidine dimers that inhibit transcription and replication and can lead to single-stranded breaks in the sugar-phosphate backbone (22). Indirect effects of UVR occur through the generation of reactive oxygen species (ROS), which can induce single- and double- strand breaks, apurinic sites, and base damage in DNA, as well as the oxidation and chemical modification of proteins and lipids (23). Bacterial tolerance to UV is conferred by a complex network of genetic and physiological systems termed the "UV-resistome", which has five basic functions: sense, shield, detoxify, repair, and tolerate (24). Photoreceptors and other stress sensors sense specific UV wavelengths and DNA damage, triggering a regulatory cascade that elicits specific cellular responses (25, 26). Specialized membrane proteins and UV-absorbing pigments shield intracellular components from irradiation (27). ROS-scavengers detoxify reactive species to prevent oxidative damage and maintain cellular redox homeostasis (28). Efficient DNA repair proteins repair genetic damages (29). And finally, error-prone polymerases tolerate and bypass unrepaired lesions to ensure survival of the cell at the cost of introducing mutations to the genome (30). The general response of bacteria to UVR and the DNA repair strategies utilized have been well-studied in organisms such as *E. coli* (22, 29, 31). However, model species are not representative of natural bacterial populations, and in particular, those that disseminate widely in the atmosphere.

Previously, we sampled aerosols to altitudes of 38 km ASL using a specialized payload attached to a helium balloon (32), isolated a variety of bacteria from the samples, and demonstrated their high tolerance to desiccation (15-25% RH) and UVCR (λ= 254 nm) (20).

Several of the isolates displayed levels of resistance rivaling that of the highly radio- and xero-tolerant bacterium *Deinococcus radiodurans*. In this study, we sequenced the genomes of two highly tolerant isolates (*Curtobacterium* sp. L6-1 and *Noviherbaspirillum* sp. L7-7A) and used comparative genomic analyses with closely related, UV-sensitive reference strains to identify genetic features likely contributing to UVCR tolerance. We also used directed evolution of the UV-sensitive *Curtobacterium flaccumfaciens pv. flaccumfaciens* strain DSM 20129 (referred to hereafter as DSM 20129) to improve its UVCR tolerance and identified the mutations responsible for enhanced resistance. Additionally, we examined cellular ROS levels in the strains after UVCR exposure and assessed photolyase activities via an *in vivo* photorepair assay. Our results improve understanding of the mechanisms enabling bacterial survival during atmospheric transport and genetic determinants of UVR tolerance in taxa for which extreme resistance has not been previously reported or investigated.

Results

UVCR-Resistance in Stratospheric Isolates and Related Strains

Based on comparison of 16S rRNA gene sequences from strains L6-1 and L7-7A, these isolates were identified as members of the Gram-positive actinobacterial genus *Curtobacterium* and the Gram-negative betaproteobacterial genus *Noviherbaspirillum*, respectively (20). To assess whether the high UVCR tolerance observed in the isolates is a feature shared with other closely related taxa, actinobacterial and betaproteobacterial reference strains were identified (Fig. 1A), obtained from culture collections (Table A1), and screened for UVCR tolerance. The inactivation rate (k) and LD_{90} were derived from a survival curve for each strain (Table A2). *Curtobacterium* sp. L6-1 has higher UVCR tolerance (LD_{90} of 470 J m^{-2}) than DSM 20129 (LD_{90} of 98 J m^{-2}; Fig. 1B; Table S2). Similarly, *Noviherbasprillum* sp. L7-7A also displayed higher

UVCR tolerance than the reference strains tested (Fig. 1C), with an average LD_{90} of 290 J m^{-2} compared to 195 J m^{-2} for *N. soli* SUEMI10, 63 J m^{-2} for *N. autotrophicum* TSA66, and 35 J m^{-2} for *N. denitrificans* TSA40 (Table A2).

Genetic Differences Between UVCR-Tolerant and -Sensitive Strains

The disparities in UVCR tolerance between the stratospheric isolates and reference strains suggested that L6-1 and L7-7A possess genetically discernable features contributing to this phenotype. To enable comparative genomic analysis, whole genome sequences were obtained for the *Curtobacterium* and *Noviherbaspirillum* strains and deposited in GenBank (33).

Strain L6-1 has a single 3.4 Mbp circular chromosome with a GC content of 72.0% and 3,158 genes encoding 12 rRNAs, 46 tRNAs, and 3,072 proteins (Table 1). Strain DSM 20129 possesses a circular chromosome and plasmid that together total 3.8 Mbp, with a GC content of 70.9%, and 3,616 genes encoding 9 rRNAs, 47 tRNAs, and 3,517 proteins. The two strains share 83% average nucleotide identity (ANI), which is below >95% values typically observed for closely related populations in a species taxon (34–37). For the *Noviherbaspirillum* strains, L7-7A possesses three circular chromosomes consisting of 5.2 Mbp and a GC content of 62.0%, with 4,771 genes encoding 15 rRNAs, 64 tRNAs, and 4,581 proteins. Although L7-7A has a genome size and content more similar to that of strain TSA66, it shares 79% ANI with both TSA66 and TSA40 and is likely a separate species (Table 1).

To analyze DNA repair and ROS detoxification pathways of the UV-resistome, genome comparisons using the RAST annotation server and the BLAST alignment tool were performed (Tables A3 and A4 for L6-1; Tables A5 and A6 for L7-7A; respectively). L6-1 encodes four additional proteins associated with DNA repair that are not found in DSM 20129 (Fig. 2; Table A3), including endonuclease VIII (*nei2*), two homologs of the UvrD/PcrA DNA helicases

(*uvrD2* & *pcrA*), and a cryptochrome/photolyase family protein (*phr1*). In addition to DNA repair genes, L6-1 encodes a homolog of the KatA catalase (*katA*; Fig. 2; Table A4), the major catalase expressed in vegetative *Bacillus* (38), whereas DSM 20129 encodes a KatX homolog (Table A4), which has been demonstrated to protect germinating endospores from H_2O_2 stress (39). A homolog of the peroxide operon regulator PerR (*perR*) from *B. subtilis* is also found in L6-1, but not DSM 20129 (Fig. 2; Table A4). L6-1 also possesses an extra copy of the glutaredoxin-like protein NrdH (*nrdH2*; Fig. 2; Table A4) involved in disulfide reduction.

Of the nine DNA repair genes identified in L7-7A that are absent in strains TSA40 and TSA66 (Fig. 3; Table A5), there are additional copies of endonuclease III (*nth2* & *nth3*) and excinuclease UvrABC subunit A (*uvrA2*), along with the RecBCD nuclease subunit D (*recD*), DNA ligase C (*ligC*), alpha-ketoglutarate-dependent dioxygenase AlkB (*alkB*), error prone DNA polymerase V subunit D (*umuD*), and exonuclease SbcCD (*sbcC & sbcD*). Notably, all the *Noviherbaspirillum* strains lack the *recB* and *recC* genes, as well as genes for the alternative repair protein RecF of the RecFOR recombination pathway (Table A5). In addition to LigC, other essential components of the bacterial non-homologous end joining (NHEJ) repair pathway (LigD and Ku) are present in strains L7-7A and TSA40 (Table A5). Antioxidant genes unique to L7-7A (Fig. 3; Table A6) include additional copies of catalase (*katE*), a divalent metal cation transporter (*mntH2*), and the paraquat-inducible protein A (*pqiA2*). All three *Noviherbaspirillum* strains encode an ortholog of the *B. subtilis* KatX catalase (Table A6). However, L7-7A also encodes an ortholog of the *E. coli* KatE catalase (Fig. 3; Table A6). Though strain TSA40 possesses two genes for MntH, *mntH2* has low similarity to the *mntH2* of L7-7A (Table A6) and may have a different function.

Directed Evolution of UVCR Tolerance in *C. flaccumfaciens* DSM 20129

Experiments designed to improve UVCR tolerance of the reference strains through repeated exposure to sublethal doses of UVCR (Fig. 4A) were partially successful. After 10 rounds of selection, we were unable to significantly improve the UVCR tolerance of the *Noviherbaspirillum* strains (data not shown). However, decreased UVCR sensitivity occurred incrementally in strain DSM 20129 during 12 rounds of selection, increasing its LD_{90} by 3.5-fold in comparison to the founder population and to a level comparable with isolate L6-1 (Fig. 4B).

Whole genome sequences were obtained for five evolved strains of DSM 20129 from the directed evolution experiment and where an increase in UVCR tolerance was observed (Table 2), and the mutations acquired were identified using the Breseq mutation analysis pipeline (40). In total, 40 mutations were identified in the most tolerant strain (DSM-9.3.3), with five occurring in intergenic regions, six in hypothetical genes, three in pseudogenes, and 26 in protein coding genes (Fig. 4C). Of the 26 mutations in protein coding genes, six are silent and 20 are nonsynonymous mutations (Table 2; Table A7) of proteins that participate in a wide range of reactions (Fig. 4C). The most notable are involved in DNA repair (uracil DNA glycosylase and DNA photolyase), cellular redox homeostasis (NAD(P)/FAD-dependent oxidoreductase in the thioredoxin reductase family), and the stress response (cold shock protein).

Intracellular ROS Concentrations After UVCR Exposure

Given the indirect effects of UVR exposure, we determined the concentration of ROS in the cells to assess if ROS detoxification may play a role in explaining the tolerances observed. ROS concentration before and after exposure to UVCR was monitored in isolate L6-1, the DSM 20129 parent strain, and the most UVCR-tolerant evolved strain (DSM-9.3.3) using the free radical sensing fluorescent probe H_2DCFDA. ROS concentration did not significantly increase in L6-1, DSM 20129, or DSM-9.3.3 at any of the UVCR doses tested (up to 1,980 J m^{-2}; Fig. 5A).

Identical observations were made in experiments with *D. radiodurans* R1 (Fig. 5A), which is well known for its capacity to resist and detoxify oxidative stress-generating agents (41–43). In stark contrast, ROS concentrations in *E. coli* approximately doubled after each ~1,000 J m^{-2} of UVCR exposure (Fig. 5A).

In vivo Assessment of Photolyase Activity

The contribution of photolyase to UVCR tolerance was investigated using an *in vivo* photorepair assay. Light activates photolyase for the repair of DNA photoproducts (44); therefore, its relative activity can be determined by examining the survival rate of UVCR exposed populations that recover under white light in comparison to those kept in the dark. Consistent with previous studies (45–47), post-UVCR exposure to white light increased the survival rate for all strains (Fig. 5B). Based on the interpolated LD_{90} values, there was not a significant difference in survival for DSM 20129 and DSM-9.3.3, indicating that the mutations incurred in the photolyase gene did not significantly affect DNA repair activity under the conditions tested (Fig. 5B inset). Photoreactivation of L6-1 increased the LD_{90} ~140%, which is significantly higher (P-value = 0.004; one-way ANOVA) than the ~19% increase observed for the DSM strains (Fig. 5B inset).

To determine if the second photolyase gene possessed by strain L6-1 contributes to its superior photorepair capacity, we aligned the sequences to known CPD and (6-4) photolyases. The CPD photolyases from *E. coli* (EcPhrB) and *Agrobacterium fabrum* (AfPhrA) align well with one of the photolyases found in L6-1 (*phr2*: KM842_RS02105) and the photolyase from DSM 20129 (*phr*: K0028_16065) (Fig. A1A). However, the additional photolyase in L6-1 (*phr1*: KM842_RS01465) is more closely related (~37% identity) to the bacterial (6-4) photolyases of *A. fabrum* (AfPhrB), *Cereibacter sphaeroides* (CsCryB), and *Vibrio cholerae* (Vc(6–4) FeS-

BCP), and the active site residues determined for AfPhrB are largely conserved in all four species (Fig. A1B). Furthermore, the protein structural prediction algorithm AlphaFold2 was used to model 3D structures for the L6-1 and DSM 20129 photolyases with a high degree of confidence (Fig. A2A-C). 3D structural alignments with the *E. coli* CPD photolyase (EcPhrB, PDB ID: 1DNP) show high similarity with the L6-1 Phr2 and DSM 20129 Phr, with a template-modeling score (TM-score) of 0.87 for both proteins (Fig. A3A). The L6-1 Phr1 shows high similarity with the *A. fabrum* (6-4) photolyase (AfPhrB, PDB ID: 5KCM) with a TM-score of 0.89, further supporting its proposed function as a bacterial (6-4) photolyase (Fig. A3B).

To assess the contributions of *phr1* and *phr2* to survival under UVCR exposure, we cloned them into expression vectors for heterologous expression in *E. coli* BL21 cells. Wild type BL21 cells were rapidly inactivated upon UVCR exposure, with an LD_{90} of 16 J m^{-2} under photoreactivating conditions (Fig. A4A). Overexpression of the native *E. coli* CPD photolyase (EcPhrB) significantly increased the LD_{90} by more than 230% during photoreactivation (Fig. A4B). Photoreactivation by the putative CPD photolyases from the *Curtobacterium* strains (L6Phr2 and DSMPhr for L6-1 *phr2* and DSM 20129 *phr*, respectively) also improved the survival of BL21, increasing the LD_{90} by 330% and 270%, respectively (Fig. A4B). In contrast, expression of the putative (6-4) photolyase from strain L6-1 (L6Phr1) alone did not significantly improve UVCR survival of BL21 cells (Fig. A4B). However, when the two L6-1 photolyases were co-expressed (L6Phr1 + L6Phr2), photoreactivation significantly improved survival over L6Phr2 alone (Fig. A4B) and increased the LD_{90} by an average of 400%.

Discussion

There is a strong gradient of increasing biological stressors with altitude in the atmosphere (48, 49), and under the extreme environmental conditions in the stratosphere,

prolonged exposure to UVR and desiccation are most important to limiting survival (18, 19, 50–61). The bacterial isolates studied (*Curtobacterium* sp. L6-1 and *Noviherbaspirillum* sp. L7-7A) were isolated from aerosols sampled at altitudes of 18 to 29 km ASL in New Mexico, USA and investigated because of their high tolerance to UVCR and desiccation (20). We tested close phylogenetic relatives of these isolates and found that they do not have extraordinary tolerance to UVCR (Fig. 1), providing an opportunity for a comparative analysis. UVR-induced cellular damage occurs directly through dimerization of pyrimidine bases in DNA, and indirectly, through the ROS generated by photosensitization mechanisms (31, 62). Accordingly, we hypothesized that higher tolerance to UVCR by isolates from the stratosphere is due to possessing DNA repair and antioxidant genes not found in their sensitive relatives.

Comparative genomic evidence for UVR tolerance in Noviherbaspirillum sp. L7-7A

To our knowledge, UVR tolerance in the genus *Noviherbaspirillum* has not been previously reported or examined. Though we were unable to improve UVCR tolerance in the *Noviherbaspirillum* reference strains through directed evolution, comparative genomic analyses identified 12 genes in isolate L7-7A involved in DNA repair and antioxidant systems that were not present in the *Noviherbaspirillum* reference strain genomes (Fig. 3; Tables A5-A6): *nth2*, *nth3*, *uvrA2*, *recD*, *ligC*, *alkB*, *umuD*, *sbcC*, *sbcD*, *katE*, *mntH2*, and *pqiA2*. Previous studies have implicated a role for these genes in UVCR tolerance (Supplemental Discussion), and as such, any one (or combination) of these 12 genes could be responsible for isolate L7-7A's high UVCR tolerance. However, genes with unknown functions (~21% of ORFs in the L7-7A genome) cannot be ruled out as contributing to this phenotype.

Genetic basis of UVR tolerance in the Curtobacterium strains

Previous studies have documented high UVR tolerance in members of the *Curtobacterium*, implying that it may be a common phenotype in this genus. Sundin and Jacobs (63) examined UVCR tolerance in bacteria isolated from the phyllosphere of field-grown peanut plants and found that *Curtobacterium* strains represented the largest proportion (~43%, n=213) of those with UVCR minimum inhibitory doses (MID_c) greater than 150 J m^{-2}. Highly UVCR resistant strains of *Curtobacterium* have also been isolated from desert rock varnish, with 17% remaining viable after a UVCR dose of 220 J m^{-2} (64). Our results are consistent with these studies, with even the most UVCR "sensitive" *Curtobacterium* strain (DSM 20129) having an LD_{90} of ~100 J m^{-2}. Notably, *Curtobacterium* sp. L6-1 has a UVCR LD_{90} of 470 J m^{-2}, which is more than double of that reported for other members of this genus and near survival rates reported for *D. radiodurans* (660 J m^{-2}; (65)). In general, a species' tolerance to UVR approximates natural exposure (24), which makes high tolerance to UVCR a surprising phenotype for populations to maintain in surface environments. However, this phenotype would be highly relevant for enabling survival and persistence at high altitudes in the atmosphere (20).

Comparative genomic analyses with DSM 20129 showed that strain L6-1 possesses seven additional genes related to DNA repair and antioxidant systems (Fig. 2; Tables A3-A4): *nei2*, *uvrD2*, *pcrA*, *phr1*, *katA*, *perR*, and *nrdH2*. Endonuclease VIII (*nei2*) is a bifunctional DNA N-glycosylase and abasic (AP) site lyase involved in the BER pathway. It initiates DNA repair by recognizing and removing oxidative base lesions and cleaving the phosphodiester backbone of the resulting AP site (66, 67). The UvrD DNA helicase II protein unwinds DNA in the 3′-5′ direction and plays a critical role in recombination, NER, and MMR (68–70). PcrA is a homolog of the UvrD helicase found in Gram-positive bacteria and has also been shown to participate in repairing UVR-induced DNA damage in *Bacillus* species (71).

Glutaredoxins (Grx) and glutathione (GSH), the main nonenzymatic antioxidants in Gram-negative bacteria, are generally absent in Gram-positive species. Many actinobacterial species are known to possess an alternative antioxidant system involving mycothiol (MSH), a low molecular weight thiol (72). Both L6-1 and DSM 20129 possess homologs for the *mshA-D* operon of the MSH biosynthesis pathway, and thus, MSH may serve as an important antioxidant in these strains. An additional copy of the gene encoding glutaredoxin-like protein NrdH in strain L6-1 is notable as NrdH has been shown to perform similar functions as the Grx/GSH system and is reducible by thioredoxin reductase (73, 74), an enzyme ubiquitous in all domains of life. In the GSH-lacking bacterium *Corynebacterium glutamicum*, NrdH enhances oxidative stress resistance (75), suggesting the second *nrdH* gene in L6-1 could play a similar role.

Cross-tolerance to environmental stress

Desiccation- and radio-tolerance phenotypes frequently co-occur in extremophilic bacteria and archaea (76–84). Given that the acute doses to which radiotolerant species are resistant greatly exceed natural ionizing radiation sources on Earth, there is no evolutionary basis for ionizing radiation resistance to arise through natural selection. Studies have demonstrated a genetic linkage between desiccation- and ionizing radiation-resistance in *D. radiodurans* R1, supporting the hypothesis that DNA repair mechanisms evolved to compensate for water loss are also highly effective at repairing the similar pattern of DNA damage produced by exposure to ionizing radiation (85). Similarly, there is no obvious fitness benefit to having high UVCR resistance in any modern environment on Earth besides the stratosphere. However, since water stress is a very common phenomenon in the biosphere, the genetic and biochemical mechanisms that enhance survival to desiccation (e.g., ROS detoxification) may also provide tolerance to UVCR. Further, when L6-1 and L7-7A are desiccated (25% RH) and exposed to UVCR, their

294 LD_{90}s are 1200 J m^{-2} and 580 J m^{-2}, respectively (20). These rates of survival are 2- to 3-fold
295 higher than those observed when water has not been actively removed from the cells (Table A2)
296 and highlights another protective effect that desiccation resistance can provide against indirect
297 effects of UVR exposure.

298 In addition to possessing efficient pathways for repairing DNA damage, the ionizing and
299 UVCR 'resistome' also includes mechanisms to physiologically detoxify ROS generated during
300 exposure to these high-energy wavelengths. ROS produced when cells are exposed to UVR or
301 desiccated can oxidize lipids and proteins (86, 87), as well as react with many other cellular
302 constituents to inflict damage. ROS detoxification is known to have a role in bacterial
303 desiccation resistance (87) and radiosensitive strains of *D. radiodurans* are more susceptible to
304 oxidative damage than radiotolerant strains (88). Oxidative stress is a major contributor to the
305 damage caused by desiccation and radiation; therefore, efficient antioxidant systems are likely to
306 be important traits of xero- and radio-tolerant species. Our experiments indicate the presence of
307 efficient ROS detoxification mechanisms in L6-1 and DSM 20129, with neither showing any
308 significant increases in intracellular ROS concentrations after UVCR exposure (Fig. 5A). This
309 implies other members of the *Curtobacterium* could also possess this trait, a contention
310 supported by a study that exposed phyllosphere communities to the highly oxidative compound
311 ozone (5,000-10,000 ppb) and found that the relative abundance of *Curtobacterium* taxa
312 increased by ~4-fold, implying a high tolerance of ozone (89). Consequently, it is tempting to
313 speculate on the role that microbial antioxidant mechanisms may play during stratospheric
314 transport beyond enhancing microbial tolerance to UVR and desiccation, as the concentration of
315 ozone at altitudes of 15 to 30 km ASL (~1,000 to 8,000 ppb) is ~1000-fold higher than air near
316 the surface (90).

Photoprotection strategies in Curtobacterium

The comparative genomics analysis and directed evolution experiments implicated photolyase family proteins in providing increased UVCR tolerance in the *Curtobacterium* strains (Figs. 2 and 4C; Table 2). In bacteria, UVR-induced DNA dimers are repaired through direct reversal by photolyases or the lesion is removed via the NER pathway. NER requires the coordinated action of multiple proteins for incision, unwinding, and excision of a damage-containing segment of DNA, followed by resynthesis and ligation of the excised nucleotides (22, 29, 91). However, because this is an energy-intensive process, a more measured response may be necessary if a generous supply of energy is not available to the cell. For instance, direct reversal of DNA photoproducts by photolyases requires a single protein and light. Given the opportunity to function, the selective advantages of the photolyase repair system would make it a trait favorable to any species in an energy limited, high UVR flux environment, including the high atmosphere.

Photolyases catalyze the direct reversal of pyrimidine dimers in DNA when activated with near-UV/blue light in a process called photoreactivation (44). Two major classes of DNA photoproducts are produced by UVR: cyclobutane pyrimidine dimers (CPD) and pyrimidine (6-4) pyrimidone photoproducts (6-4PP). Direct repair of these lesions is catalyzed by photolyases specific to each lesion type (44, 92). Though CPD photolyases are widespread amongst bacteria, only three bacterial (6-4) photolyases have been characterized to date: PhrB of *Agrobacterium fabrum* (45, 93) (formerly *Agrobacterium tumefaciens* (94)), CryB of *Cereibacter sphaeroides* (95, 96) (formerly *Rhodobacter sphaeroides* (97)), and Vc(6–4) FeS-BCP of *Vibrio cholerae* (98). However, phylogenetic comparison with photolyase genes in the eukaryotic cryptochrome/photolyase family suggests that (6-4) photolyases are more prevalent in

prokaryotes than initially thought (93). Sequence alignments and predicted structural models of the L6-1 photolyases (Fig. A1) suggest it possesses a putative CPD photolyase (*phr2*: KM842_RS16065) and (6-4) photolyase (*phr1*: KM842_RS01465). Strain L6-1 has higher photorepair capacity than strain DSM 20129 (Fig. 5B), which only possesses a CPD photolyase.

To demonstrate functionality of the putative 6-4PP and CPD photolyases of L6-1, *phr1* and *phr2*, respectively, were heterologously expressed in *E. coli* and their effects on its UVCR tolerance were examined. Although expression of *phr1* did not increase UVCR tolerance over that observed in the control, expression of *phr2* increased survival by ~325%, while co-expression of *phr1* and *phr2* increased the survival rate even further (Fig. A4). These results are likely due to the larger number of CPD lesions (75-90% of total) upon UV exposure as compared to 6-4PP generated (22, 99–101). If further study shows the L6-1 *phr1* to be a bona fide (6-4) photolyase, its activity alone might be expected to have a negligible effect on cell survival since the overwhelming amount of DNA damage would be CPD dimers. However, when *phr1* and *phr2* are co-expressed, the repair of both CPD and 6-4PP dimers has a synergistic effect on survival.

Conclusion

We investigated the genetic basis for extreme UVCR resistance phenotypes in bacteria recovered from stratospheric air masses (20), where high UVCR fluxes and low water availability represent endmember values for these variables in the biosphere. Recognizing the genetic underpinnings for the expressed characteristics mitigating damage from UVCR was facilitated by the rich history of experimental work that has characterized the biochemistry and molecular biology of DNA repair processes in model organisms. In fact, the genomes of the proteobacterial and actinobacterial strains studied encode genes for most, if not all, of the typical

363 complement of DNA repair proteins documented in *E. coli* and many other bacteria. This
364 indicates that strains L7-7A and L6-1 operate their canonical DNA repair pathways in a manner
365 more effective than other species and/or that survival to UVCR is enhanced through alternative
366 mechanisms. For microbial species surviving long distance dispersal as aerosols in the
367 atmosphere, efficient DNA repair systems, such as photoreactivation, and mechanisms that
368 evolved to cope with water stress are likely to be valuable for enduring the high UVR fluxes that
369 intensify with altitude.

370 **Materials and Methods**

371 ***Bacterial Strains and Culture Conditions***

372 The bacterial strains used in this study are listed in Table A1. *Curtobacterium* sp. L6-1 and
373 *Noviherbaspirillum* sp. L7-7A were isolated from aerosols collected using a helium balloon
374 payload that sampled at altitudes of 18 to 23 km and 24 to 29 km ASL, respectively, near Ft.
375 Sumner, New Mexico in 2013 (32). Reference strains phylogenetically related to isolates L6-1
376 and L7-7A and that were identified as available in culture collections were obtained from the
377 German Collection of Microorganisms and Cell Cultures (DSMZ) and the United States
378 Department of Agriculture (USDA) Agricultural Research Service Culture Collection (NRRL).
379 These included *Curtobacterium flaccumfaciens pv. flaccumfaciens* (DSM 20129), *Mycetocola*
380 *reblochoni* (LMG 22367), *Plantibacter flavus* (DSM 14012T), and *Noviherbaspirillum soli*
381 (SUEMI10). *Noviherbaspirillum denitrificans* (TSA40) and *Noviherbasprillum autotrophicum*
382 (TSA66) were kindly provided by Dr. Satoshi Ishii of the University of Minnesota. Unless
383 otherwise noted, the actinobacterial and betaproteobacterial strains were cultured aerobically at
384 30°C with vigorous shaking in LB (10 g L^{-1} tryptone, 5 g L^{-1} yeast extract, 10 g L^{-1} NaCl) and
385 R2A (Difco cat. no.: 218262) media, respectively. When required, media were amended with

386 antibiotics at the following concentrations: spectinomycin (50 µg mL^{-1}) & carbenicillin (100 µg
387 mL^{-1}).

388 ***UVCR Survival Assays***

389 Cultures were grown in 5 mL of liquid media to stationary phase, and six serial dilutions of this
390 material were prepared in 10 mM $MgSO_4$. Ten µL of each dilution was transferred to six sections
391 of a square plate containing agar-solidified growth media. Portions of the plate were then
392 covered with aluminum foil such that sections uncovered sequentially during 1 min interval
393 exposures were provided with controlled doses of UVCR (GE G36T5 UVC Light Bulb; λ = 254
394 nm; 3.3 W m^{-2}) that were 198, 396, 594, 792, and 990 J m^{-2}. The UVCR dose was measured
395 using a digital radiometer (Solar Light Company, Inc., Glenside, PA). The longest exposure for
396 the populations was 5 min. and the section of the plate that remained covered during the
397 experiment (i.e., was not exposed to UVCR) served as the control (N_0). The cultures were
398 incubated at 30°C for 24 to 48 h and the number of colony forming units (CFU) surviving each
399 UVCR dose (N) was used to calculate the surviving fraction, expressed as N/N_0. Survival rates
400 are reported as the mean and SEM for three biological replicates.

401 ***Whole Genome Sequencing and Comparative Genomics***

402 Whole genome sequences for *Noviherbaspirillum sp.* L7-7A, *Curtobacterium sp.* L6-1, and
403 *Curtobacterium flaccumfaciens* strain DSM 20129 were obtained as described previously (33).
404 Briefly, stationary phase cultures were pelleted, frozen (-70°C), and shipped to SNPsaurus
405 (Eugene, OR) for DNA extraction, library preparation, sequencing, and genome assembly using
406 the PacBio Sequel II sequencing platform followed by de novo genome assembly using the Flye
407 v2.7 assembler (102). The assembled genomes were submitted to GenBank (L7-7A: JAHQRJ01;

L6-1: CP076544.1; DSM 20129: CP080395.1/CP080396.1) and annotated using the NCBI Prokaryotic Genome Annotation Pipeline (PGAP) (103).

Average nucleotide identity (ANI) and average amino acid identity (AAI) among the isolates and reference strains were calculated using the ANI and AAI calculators from the Kostas lab (http://enve-omics.ce.gatech.edu/) (104, 105). Functional comparisons were made with the Rapid Annotation using Subsystem Technology (RAST) server and the SEED Viewer (106–108). Further comparisons were made by searching for homologs of known DNA repair and ROS detoxification proteins from model organisms in the L6-1, DSM 20129, L7-7A, TSA40, and TSA66 genomes using the blastp algorithm from NCBI's Basic Local Alignment Search Tool (BLAST) (109). Query protein sequences were obtained from the UniProt database for *Escherichia coli* strain K12, *Bacillus subtilis* strain 168, and *Mycobacterium tuberculosis* strain ATCC 25618 / H37Rv (110). Reciprocal best hits were considered homologs if the bit score was >50, E-value was <1e-5, and query coverage was >50% (111). Differences in gene content among the isolates and the reference strain relatives were visualized using the BLAST Ring Image Generator (BRIG) (112).

Directed Evolution and Mutation Analysis

The survival of strain DSM 20129 to UVCR exposure was determined as described above. Triplicate colonies surviving the highest UVCR dose were selected, grown separately in liquid media, exposed to UVCR (as described in the section "UVCR Survival Assays" above), and the process was repeated a total of 12 times (Fig. 4A). The populations from each cycle of exposure were archived by freezing aliquots of the cultures in 25% glycerol and storing at -70°C. Genome sequences were obtained for select strains throughout the directed evolution process using the Illumina NextSeq 2000 sequencing platform (Microbial Genome Sequencing Center,

Pittsburgh, PA) with 2×150 bp reads. Sequencing reads were quality filtered and adaptors trimmed using the Trim Galore script (113), followed by mapping to the reference genome and mutation identification with the Breseq mutation analysis pipeline (40). The ancestral parent strain was sequenced and used as a control to correct the reference genome before comparison with the evolved strains. Gene Ontology (GO) functional annotations for proteins incurring mutations throughout the directed evolution process were obtained using Blast2GO (114).

ROS Quantification Assays

The free radical probe 2',7'-dichlorodihydrofluoresceindiacetate (H_2DCFDA) (Biotium, Fremont, CA) was used to quantify ROS. Stationary phase cultures of *E. coli* MG1655, *D. radiodurans* R1, isolate L6-1, the wild-type parent strain DSM 20129, and UV-evolved strain DSM-9.3.3 were diluted to OD_{600} 1.0 in 10 mL of media. Cells were washed with 10 mM potassium phosphate buffer (pH 7.0) and incubated for 30 min at 25°C in the same buffer containing 10 μM H_2DCFDA. Subsequently, cells were washed and resuspended in 10 mL potassium phosphate buffer (10 mM; pH 7.0), transferred to 60×15 mm petri plates, and exposed to UVCR doses of 0, 990, or 1,980 J m^{-2} while stirring the cell suspensions at 400 rpm with a magnetic stir bar. The exposed cell populations were then washed, resuspended in fresh buffer, and disrupted by vortexing with lysing matrix B (MP Biomedicals). Cellular debris was removed by centrifugation for 10 min at 5,000×g, and fluorescence intensity in the supernatant was measured using a multi-well plate reader (Molecular Devices SpectraMax M3; Exc. 490nm, Emm. 519nm). The amount of fluorescence observed was normalized per mg of protein, as determined by the Pierce BCA Protein Assay Kit (Thermo Scientific) and compared relative to data from the unexposed control (i.e., time zero is 100% fluorescence intensity). Values reported are the average of three biological replicates and the error bars indicate SEM.

Photolyase Activity Assays and Sequence/Structural Comparisons

To assess *in vivo* photorepair, isolate L6-1, the DSM 20129 founder strain, and UV-evolved strain DSM-9.3.3 were grown to stationary phase and exposed to UVCR using the same method as described for the UVCR survival assays. After exposure, half of the cultures were immediately placed in the dark and the other half were photoreactivated for 1 h under a daylight lamp (GE F20T12-C50-ECO 20W Chroma 50 5000K Ecolux Daylight Light Bulb). All of the cultures were subsequently incubated in the dark at 30°C until colonies formed. Survival rates under dark and light conditions were calculated, and the lethal dose reducing the population by 90% (LD_{90}) was determined by fitting the survival curves to an exponential decay model. The percent increase in LD_{90} by photoreactivation was calculated using the equation: $\frac{LD90_{Light}-LD90_{Dark}}{LD90_{Dark}} \times 100 = \%\, Increase$. Results shown represent the average of four biological replicates with error bars representing SEM.

Acknowledgements

This work was supported by funding from the University of Florida Institute of Food and Agricultural Sciences and awards from the National Aeronautics and Space Administration (NASA) Exobiology Program (80NSSC21K0486) and the University of Central Florida NASA Florida Space Grant Consortium and Space Florida (NNX15034). B.C.C. is indebted to John R. Battista for enduring countless discussions on bacterial radio- and desiccation-tolerance. Satoshi Ishii of the University of Minnesota kindly provided strains for the analysis. We thank Madison Drum for assistance with the directed evolution experiments. We also thank T. Gregory Guzik, Noelle Bryan, Doug Granger, Michael Stewart, and the many other dedicated members of the 2009-2013 ACES and HASP balloon programs at Louisiana State University for their tireless efforts in developing/testing the aerosol sampling payloads, conducting the missions (and their

recovery, no matter where it landed!), and performing the initial research that made this study possible.

References

1. Douwes J, Thorne P, Pearce N, Heederik D. 2003. Bioaerosol health effects and exposure assessment: progress and prospects. Ann Occup Hyg 47:187–200.

2. Kim KH, Kabir E, Jahan SA. 2018. Airborne bioaerosols and their impact on human health. J Environ Sci (China) 67:23.

3. Dillon CF, Dillon MB. 2020. Multiscale Airborne Infectious Disease Transmission. Appl Environ Microbiol 87:e02314–e02320.

4. Yadav S, Gettu N, Swain B, Kumari K, Ojha N, Gunthe SS. 2020. Bioaerosol impact on crop health over India due to emerging fungal diseases (EFDs): an important missing link. Environ Sci Pollut Res Int 27:12802–12829.

5. Brown JKM, Hovmøll MS. 2002. Aerial dispersal of pathogens on the global and continental scales and its impact on plant disease. Science 297:537–541.

6. Phillips VTJ, Andronache C, Christner B, Morris CE, Sands DC, Bansemer A, Lauer A, McNaughton C, Seman C. 2009. Potential impacts from biological aerosols on ensembles of continental clouds simulated numerically. Biogeosciences 6:987–1014.

7. Joyce RE, Lavender H, Farrar J, Werth JT, Weber CF, D'Andrilli J, Vaitilingom M, Christnera BC. 2019. Biological Ice-Nucleating Particles Deposited Year-Round in Subtropical Precipitation. Appl Environ Microbiol 85:1567–1586.

8. Fröhlich-Nowoisky J, Kampf CJ, Weber B, Huffman JA, Pöhlker C, Andreae MO, Lang-Yona N, Burrows SM, Gunthe SS, Elbert W, Su H, Hoor P, Thines E, Hoffmann T, Després VR, Pöschl U. 2016. Bioaerosols in the Earth system: Climate, health, and ecosystem interactions. Atmos Res 182:346–376.

9. Smith DJ, Griffin DW, McPeters RD, Ward PD, Schuerger AC. 2011. Microbial survival in the stratosphere and implications for global dispersal. Aerobiologia (Bologna) 27:319–332.

10. Smith DJ. 2013. Microbes in the upper atmosphere and unique opportunities for astrobiology research. Astrobiology 13:981–990.

11. Maki T, Hara K, Kobayashi F, Kurosaki Y, Kakikawa M, Matsuki A, Chen B, Shi G, Hasegawa H, Iwasaka Y. 2015. Vertical distribution of airborne bacterial communities in an Asian-dust downwind area, Noto Peninsula. Atmos Environ 119:282–293.

12. Els N, Baumann-Stanzer K, Larose C, Vogel TM, Sattler B. 2019. Beyond the planetary boundary layer: Bacterial and fungal vertical biogeography at Mount Sonnblick, Austria. Geo 6:e00069.

13. Burrows SM, Butler T, Jöckel P, Tost H, Kerkweg A, Pöschl U, Lawrence MG. 2009. Bacteria in the global atmosphere - Part 2: Modeling of emissions and transport between different ecosystems. Atmos Chem Phys 9:9281–9297.

14. Rodriguez-Manfredi JA, de la Torre Juarez M, Sanchez-Lavega A, Hueso R, Martinez G, Lemmon MT, Newman CE, Munguira A, Hieta M, Tamppari LK, Polkko J, Toledo D, Sebastian E, Smith MD, Jaakonaho I, Genzer M, De Vicente-Retortillo A, Viudez-Moreiras D, Ramos M, Saiz-Lopez A, Lepinette A, Wolff M, Sullivan RJ, Gomez-Elvira J, Apestigue V, Conrad PG, Del Rio-Gaztelurrutia T, Murdoch N, Arruego I, Banfield D, Boland J, Brown AJ, Ceballos J, Dominguez-Pumar M, Espejo S, Fairén AG, Ferrandiz R, Fischer E, Garcia-Villadangos M, Gimenez S, Gomez-Gomez F, Guzewich SD, Harri AM, Jimenez JJ, Jimenez V, Makinen T, Marin M, Martin C, Martin-Soler J, Molina A, Mora-Sotomayor L, Navarro S, Peinado V, Perez-Grande I, Pla-Garcia J, Postigo M, Prieto-Ballesteros O, Rafkin SCR, Richardson MI, Romeral J, Romero C, Savijärvi H, Schofield JT, Torres J, Urqui R, Zurita S. 2023. The diverse meteorology of Jezero crater over the first 250 sols of Perseverance on Mars. Nat Geosci 16:19–28.

15. Polkko J, Hieta M, Harri A-M, Tamppari L, Martínez G, Viúdez-Moreiras D, Savijärvi H, Conrad P, Mier MPZ, Juarez MDLT, Hueso R, Munguira A, Leino J, Gómez F, Jaakonaho I, Fischer E, Genzer M, Apestigue V, Arruego I, Banfield D, Lepinette A, Paton M, Rodriguez-Manfredi JA, Lavega AS, Sebastian E, Toledo D, Vicente-Retortillo A. 2023. Initial Results of the Relative Humidity Observations by MEDA Instrument Onboard the Mars 2020 Perseverance Rover. J Geophys Res Planets 128:e2022JE007447.

16. Smith DJ, Thakrar PJ, Bharrat AE, Dokos AG, Kinney TL, James LM, Lane MA, Khodadad CL, Maguire F, Maloney PR, Dawkins NL. 2014. A Balloon-Based Payload for Exposing Microorganisms in the Stratosphere (E-MIST). Gravitational and Space Research 2:70–80.

17. Smith DJ, Sowa MB. 2017. Ballooning for Biologists: Mission Essentials for Flying Life Science Experiments to Near Space on NASA Large Scientific Balloons. Gravit Space Res 5:52.

18. Pulschen AA, de Araujo GG, de Carvalho ACSR, Cerini MF, de Mendonça Fonseca L, Galante D, Rodrigues F. 2018. Survival of Extremophilic Yeasts in the Stratospheric Environment during Balloon Flights and in Laboratory Simulations. Appl Environ Microbiol 84.

19. Cortesão M, Siems K, Koch S, Beblo-Vranesevic K, Rabbow E, Berger T, Lane M, James L, Johnson P, Waters SM, Verma SD, Smith DJ, Moeller R. 2021. MARSBOx: Fungal and Bacterial Endurance from a Balloon-Flown Analog Mission in the Stratosphere. Front Microbiol 12:601713.

20. Bryan NC, Christner BC, Guzik TG, Granger DJ, Stewart MF. 2019. Abundance and survival of microbial aerosols in the troposphere and stratosphere. ISME Journal 13:2789–2799.

21. Kerr JB, Fioletov VE. 2008. Surface ultraviolet radiation. Atmosphere-Ocean 46:159–184.

22. P. Sinha R, Donat-P. Häder. 2002. UV-induced DNA damage and repair: a review. Photochemical & Photobiological Sciences 1:225–236.

23. Pattison DI, Davies MJ. 2006. Actions of ultraviolet light on cellular structures. EXS (96):131–157.

24. Kurth D, Belfiore C, Gorriti MF, Cortez N, Farias ME, Albarracín VH. 2015. Genomic and proteomic evidences unravel the UV-resistome of the poly-extremophile Acinetobacter sp. Ver3. Front Microbiol 6.

25. Takano H, Obitsu S, Beppu T, Ueda K. 2005. Light-Induced Carotenogenesis in Streptomyces coelicolor A3(2): Identification of an Extracytoplasmic Function Sigma Factor That Directs Photodependent Transcription of the Carotenoid Biosynthesis Gene Cluster. J Bacteriol 187:1825.

26. Ávila-Pérez M, Hellingwerf KJ, Kort R. 2006. Blue Light Activates the σB-Dependent Stress Response of Bacillus subtilis via YtvA. J Bacteriol 188:6411.

27. Gao Q, Garcia-Pichel F. 2011. Microbial ultraviolet sunscreens. Nat Rev Microbiol 9:791–802.

28. Lemire J, Alhasawi A, Appanna VP, Tharmalingam S, Appanna VD. 2017. Metabolic defence against oxidative stress: the road less travelled so far. J Appl Microbiol 123:798–809.

29. Goosen N, Moolenaar GF. 2008. Repair of UV damage in bacteria. DNA Repair (Amst) 7:353–379.

30. Tang M, Shen X, Frank EG, O'Donnell M, Woodgate R, Goodman MF. 1999. UmuD′2C is an error-prone DNA polymerase, Escherichia coli pol V. Proc Natl Acad Sci U S A 96:8919–8924.

31. Rastogi RP, Richa, Kumar A, Tyagi MB, Sinha RP. 2010. Molecular Mechanisms of Ultraviolet Radiation-Induced DNA Damage and Repair. J Nucleic Acids 2010:32.

32. Bryan NC, Stewart M, Granger D, Guzik TG, Christner BC. 2014. A method for sampling microbial aerosols using high altitude balloons. J Microbiol Methods 107:161–168.

33. Ellington AJ, Bryan NC, Christner BC, Reisch CR. 2021. Draft Genome Sequences of Actinobacterial and Betaproteobacterial Strains Isolated from the Stratosphere. Microbiol Resour Announc 10:e1009-21.

34. Richter M, Rosselló-Móra R. 2009. Shifting the genomic gold standard for the prokaryotic species definition. Proc Natl Acad Sci 106:19126–19131.

35. Kim M, Oh H-S, Park S-C, Chun J. 2014. Towards a taxonomic coherence between average nucleotide identity and 16S rRNA gene sequence similarity for species demarcation of prokaryotes. Int J Syst Evol Microbiol 64:346–351.

587 36. Jain C, Rodriguez-R LM, Phillippy AM, Konstantinidis KT, Aluru S. 2018. High
588 throughput ANI analysis of 90K prokaryotic genomes reveals clear species boundaries.
589 Nat Commun 9:1–8.

590 37. Ciufo S, Kannan S, Sharma S, Badretdin A, Clark K, Turner S, Brover S, Schoch CL,
591 Kimchi A, DiCuccio M. 2018. Using average nucleotide identity to improve taxonomic
592 assignments in prokaryotic genomes at the NCBI. Int J Syst Evol Microbiol 68:2386–
593 2392.

594 38. Bagyan I, Casillas-Martinez L, Setlow P. 1998. The katX gene, which codes for the
595 catalase in spores of Bacillus subtilis, is a forespore-specific gene controlled by σ(F), and
596 katX is essential for hydrogen peroxide resistance of the germinating spore. J Bacteriol
597 180:2057–2062.

598 39. Bol DK, Yasbin RE. 1991. The isolation, cloning and identification of a vegetative
599 catalase gene from Bacillus subtilis. Gene 109:31–37.

600 40. Deatherage DE, Barrick JE. 2014. Identification of mutations in laboratory-evolved
601 microbes from next-generation sequencing data using breseq. Methods in Molecular
602 Biology 1151:165–188.

603 41. Daly MJ, Gaidamakova EK, Matrosova VY, Vasilenko A, Zhai M, Leapman RD, Lai B,
604 Ravel B, Li SMW, Kemner KM, Fredrickson JK. 2007. Protein oxidation implicated as
605 the primary determinant of bacterial radioresistance. PLoS Biol 5:769–779.

606 42. Daly MJ, Gaidamakova EK, Matrosova VY, Kiang JG, Fukumoto R, Lee DY, Wehr NB,
607 Viteri GA, Berlett BS, Levine RL. 2010. Small-molecule antioxidant proteome-shields in
608 Deinococcus radiodurans. PLoS One 5:10–15.

609 43. Krisko A, Radman M. 2010. Protein damage and death by radiation in Escherichia coli
610 and Deinococcus radiodurans. Proc Natl Acad Sci U S A 107:14373–14377.

611 44. Sancar A. 1994. Structure and function of DNA photolyase. Biochemistry 33:2–9.

612 45. Oberpichler I, Pierik AJ, Wesslowski J, Pokorny R, Rosen R, Vugman M, Zhang F,
613 Neubauer O, Ron EZ, Batschauer A, Lamparter T. 2011. A Photolyase-Like Protein from
614 Agrobacterium tumefaciens with an Iron-Sulfur Cluster. PLoS One 6:e26775.

615 46. Marizcurrena JJ, Morel MA, Braña V, Morales D, Martinez-López W, Castro-Sowinski S.
616 2017. Searching for novel photolyases in UVC-resistant Antarctic bacteria. Extemophiles
617 21:409–418.

618 47. Portero LR, Alonso-Reyes DG, Zannier F, Vazquez MP, Farías ME, Gärtner W,
619 Albarracín VH. 2019. Photolyases and Cryptochromes in UV-resistant Bacteria from
620 High-altitude Andean Lakes. Photochem Photobiol 95:315–330.

621 48. Aguilera Á, Diego-Castilla G de, Osuna S, Bardera R, Mendi SS, Blanco Y, González-
622 Toril E, Aguilera Á, Diego-Castilla G de, Osuna S, Bardera R, Mendi SS, Blanco Y,
623 González-Toril E. 2018. Microbial Ecology in the Atmosphere: The Last Extreme

Environment. Extremophilic Microbes and Metabolites - Diversity, Bioprospecting and Biotechnological Applications https://doi.org/10.5772/INTECHOPEN.81650.

49. Šantl-Temkiv T, Amato P, Casamayor EO, Lee PKH, Pointing SB. 2022. Microbial ecology of the atmosphere. FEMS Microbiol Rev 46:1–18.

50. Schuerger AC, Mancinelli RL, Kern RG, Rothschild LJ, McKay CP. 2003. Survival of endospores of Bacillus subtilis on spacecraft surfaces under simulated Martian environments: implications for the forward contamination of Mars. Icarus 165:253–276.

51. Tauscher C, Schuerger AC, Nicholson WL. 2006. Survival and Germinability of Bacillus subtilis Spores Exposed to Simulated Mars Solar Radiation: Implications for Life Detection and Planetary Protection. Astrobiology 6:592–605.

52. Schuerger AC, Richards JT, Newcombe DA, Venkateswaran K. 2006. Rapid inactivation of seven Bacillus spp. under simulated Mars UV irradiation. Icarus 181:52–62.

53. Cockell CS, Schuerger AC, Billi D, Friedmann EI, Panitz C. 2005. Effects of a Simulated Martian UV Flux on the Cyanobacterium, Chroococcidiopsis sp. 029. Astrobiology 5:127–140.

54. Diaz B, Schulze-Makuch D. 2006. Microbial Survival Rates of Escherichia coli and Deinococcus radiodurans Under Low Temperature, Low Pressure, and UV-Irradiation Conditions, and Their Relevance to Possible Martian Life. Astrobiology 6:332–347.

55. de la Vega UP, Rettberg P, Reitz G. 2007. Simulation of the environmental climate conditions on Martian surface and its effect on Deinococcus radiodurans. Advances in Space Research 40:1672–1677.

56. Fendrihan S, Bérces A, Lammer H, Musso M, Rontó G, Polacsek TK, Holzinger A, Kolb C, Stan-Lotter H. 2009. Investigating the Effects of Simulated Martian Ultraviolet Radiation on Halococcus dombrowskii and Other Extremely Halophilic Archaebacteria. Astrobiology 9:104–112.

57. Peeters Z, Vos D, ten Kate IL, Selch F, van Sluis CA, Sorokin DY, Muijzer G, Stan-Lotter H, van Loosdrecht MCM, Ehrenfreund P. 2010. Survival and death of the haloarchaeon Natronorubrum strain HG-1 in a simulated Martian environment. Advances in Space Research 46:1149–1155.

58. Johnson AP, Pratt LM, Vishnivetskaya T, Pfiffner S, Bryan RA, Dadachova E, Whyte L, Radtke K, Chan E, Tronick S, Borgonie G, Mancinelli RL, Rothschild LJ, Rogoff DA, Horikawa DD, Onstott TC. 2011. Extended survival of several organisms and amino acids under simulated Martian surface conditions. Icarus 211:1162–1178.

59. Smith DJ, Schuerger AC, Davidson MM, Pacala SW, Bakermans C, Onstott TC. 2009. Survivability of Psychrobacter cryohalolentis K5 Under Simulated Martian Surface Conditions. Astrobiology 9:221–228.

60. Khodadad CL, Wong GM, James LM, Thakrar PJ, Lane MA, Catechis JA, Smith DJ. 2017. Stratosphere Conditions Inactivate Bacterial Endospores from a Mars Spacecraft Assembly Facility. Astrobiology 17:337.

61. Ye T, Wang B, Li C, Bian P, Chen L, Wang G. 2021. Exposure of cyanobacterium Nostoc sp. to the Mars-like stratosphere environment. J Photochem Photobiol 224:112307.

62. Berens PJT, Molinier J. 2020. Formation and Recognition of UV-Induced DNA Damage within Genome Complexity. Int J Mol Sci 21:1–23.

63. Sundin GW, Jacobs JL. 1999. Ultraviolet Radiation (UVR) Sensitivity Analysis and UVR Survival Strategies of a Bacterial Community from the Phyllosphere of Field-Grown Peanut (Arachis hypogeae L.). Microb Ecol 38:27–38.

64. Kuhlman KR, Allenbach LB, Ball CL, Fusco WG, la Duc MT, Kuhlman GM, Anderson RC, Stuecker T, Erickson IK, Benardini J, Crawford RL. 2005. Enumeration, isolation, and characterization of ultraviolet (UV-C) resistant bacteria from rock varnish in the Whipple Mountains, California. Icarus 174:585–595.

65. Bauermeister A, Bentchikou E, Moeller R, Rettberg P. 2009. Roles of PprA, IrrE, and RecA in the resistance of Deinococcus radiodurans to germicidal and environmentally relevant UV radiation. Arch Microbiol 191:913–918.

66. Jiang D, Hatahet Z, Melamede RJ, Kow YW, Wallace SS. 1997. Characterization of Escherichia coli Endonuclease VIII. Journal of Biological Chemistry 272:32230–32239.

67. Dizdaroglu M. 2003. Substrate specificities and excision kinetics of DNA glycosylases involved in base-excision repair of oxidative DNA damage. Mutation Research/Fundamental and Molecular Mechanisms of Mutagenesis 531:109–126.

68. Veaute X, Delmas S, Selva M, Jeusset J, Le Cam E, Matic I, Fabre F, Petit MA. 2005. UvrD helicase, unlike Rep helicase, dismantles RecA nucleoprotein filaments in Escherichia coli. EMBO J 24:180.

69. Husain I, van Houten B, Thomas DC, Abdel-Monem M, Sancar A. 1985. Effect of DNA polymerase I and DNA helicase II on the turnover rate of UvrABC excision nuclease. Proc Natl Acad Sci 82:6774–6778.

70. Dao V, Modrich P. 1998. Mismatch-, MutS-, MutL-, and helicase II-dependent unwinding from the single-strand break of an incised heteroduplex. J Biol Chem 273:9202–9207.

71. Petit MA, Dervyn E, Rose M, Entian KD, McGovern S, Ehrlich SD, Bruand C. 1998. PcrA is an essential DNA helicase of Bacillus subtilis fulfilling functions both in repair and rolling-circle replication. Mol Microbiol 29:261–273.

72. Newton GL, Arnold K, Price MS, Sherrill C, Delcardayre SB, Aharonowitz Y, Cohen G, Davies J, Fahey RC, Davis C. 1996. Distribution of thiols in microorganisms: mycothiol is a major thiol in most actinomycetes. J Bacteriol 178:1990–1995.

73. Jordan A, Åslund F, Pontis E, Reichard P, Holmgren A. 1997. Characterization of Escherichia coli NrdH: A GLUTAREDOXIN-LIKE PROTEIN WITH A THIOREDOXIN-LIKE ACTIVITY PROFILE *. Journal of Biological Chemistry 272:18044–18050.

74. Van Laer K, Dziewulska AM, Fislage M, Wahni K, Hbeddou A, Collet JF, Versées W, Mateos LM, Dufe VT, Messens J. 2013. NrdH-redoxin of Mycobacterium tuberculosis and Corynebacterium glutamicum Dimerizes at High Protein Concentration and Exclusively Receives Electrons from Thioredoxin Reductase. J Biol Chem 288:7942.

75. Si MR, Zhang L, Yang ZF, Xu YX, Liu YB, Jiang CY, Wang Y, Shen XH, Liu SJ. 2014. NrdH redoxin enhances resistance to multiple oxidative stresses by acting as a peroxidase cofactor in Corynebacterium glutamicum. Appl Environ Microbiol 80:1750–1762.

76. Moeller R, Setlow P, Reitz G, Nicholson WL. 2009. Roles of small, acid-soluble spore proteins and core water content in survival of Bacillus subtilis spores exposed to environmental solar UV radiation. Appl Environ Microbiol 75:5202–5208.

77. Singh H. 2018. Desiccation and radiation stress tolerance in cyanobacteria. J Basic Microbiol 58:813–826.

78. Romano I, Camerlingo C, Vaccari L, Birarda G, Poli A, Fujimori A, Lepore M, Moeller R, Di Donato P. 2022. Effects of Ionizing Radiation and Long-Term Storage on Hydrated vs. Dried Cell Samples of Extremophilic Microorganisms. Microorganisms 2022, Vol 10, Page 190 10:190.

79. Rainey F, Ray K, Ferreira M, Gatz B, Nobre M, Bagaley D, Rash B, Park M, Earl A, Shank N, Small A, Henk M, Battista J, Kämpfer P, da Costa M. 2005. Extensive diversity of ionizing-radiation-resistant bacteria recovered from Sonoran Desert soil and description of nine new species of the genus Deinococcus obtained from a single soil sample. Appl Environ Microbiol 71:5225–5235.

80. Slade D, Radman M. 2011. Oxidative Stress Resistance in Deinococcus radiodurans. Microbiology and Molecular Biology Reviews 75:133–191.

81. Kottemann M, Kish A, Iloanusi C, Bjork S, DiRuggiero J. 2005. Physiological responses of the halophilic archaeon Halobacterium sp. strain NRC1 to desiccation and gamma irradiation. Extremophiles 9:219–227.

82. Shukla M, Chaturvedi R, Tamhane D, Vyas P, Archana G, Apte S, Bandekar J, Desai A. 2007. Multiple-stress tolerance of ionizing radiation-resistant bacterial isolates obtained from various habitats: correlation between stresses. Curr Microbiol 54:142–148.

83. Romanovskaya VA, Rokitko P v., Mikheev AN, Gushcha NI, Malashenko YR, Chernaya NA. 2002. The Effect of γ-Radiation and Desiccation on the Viability of the Soil Bacteria Isolated from the Alienated Zone around the Chernobyl Nuclear Power Plant. Microbiology (N Y) 71:608–613.

733 84. Musilova M, Wright G, Ward JM, Dartnell LR. 2015. Isolation of Radiation-Resistant
734 Bacteria from Mars Analog Antarctic Dry Valleys by Preselection, and the Correlation
735 between Radiation and Desiccation Resistance. Astrobiology 15:1076.

736 85. Mattimore V, Battista JR. 1996. Radioresistance of Deinococcus radiodurans: functions
737 necessary to survive ionizing radiation are also necessary to survive prolonged
738 desiccation. J Bacteriol 178:633.

739 86. Santos AL, Oliveira V, Baptista I, Henriques I, Gomes NCM, Almeida A, Correia A,
740 Cunha Â. 2013. Wavelength dependence of biological damage induced by UV radiation
741 on bacteria. Arch Microbiol 195:63–74.

742 87. Fredrickson JK, Li SW, Gaidamakova EK, Matrosova VY, Zhai M, Sulloway HM,
743 Scholten JC, Brown MG, Balkwill DL, Daly MJ. 2008. Protein oxidation: key to bacterial
744 desiccation resistance? ISME J 2:393–403.

745 88. Daly MJ, Gaidamakova EK, Matrosova VY, Vasilenko A, Zhai M, Leapman RD, Lai B,
746 Ravel B, Li SMW, Kemner KM, Fredrickson JK. 2007. Protein Oxidation Implicated as
747 the Primary Determinant of Bacterial Radioresistance. PLoS Biol 5:769–779.

748 89. Liu J, Song M, Wei X, Zhang H, Bai Z, Zhuang X. 2022. Responses of Phyllosphere
749 Microbiome to Ozone Stress: Abundance, Community Compositions and Functions.
750 Microorganisms 10:680.

751 90. 2023. NASA Ozone Watch: Latest status of ozone.
752 https://ozonewatch.gsfc.nasa.gov/SH.html. Retrieved 19 March 2023.

753 91. Kisker C, Kuper J, van Houten B. 2013. Prokaryotic Nucleotide Excision Repair. Cold
754 Spring Harb Perspect Biol 5:a012591.

755 92. Todo T, Takemori H, Ryo H, Lhara M, Matsunaga T, Nikaido O, Sato K, Nomura T.
756 1993. A new photoreactivating enzyme that specifically repairs ultraviolet light-induced
757 (6-4) photoproducts. Nature 361:371–374.

758 93. Zhang F, Scheerer P, Oberpichler I, Lamparter T, Krauß N. 2013. Crystal structure of a
759 prokaryotic (6-4) photolyase with an Fe-S cluster and a 6,7-dimethyl-8-ribityllumazine
760 antenna chromophore. Proc Natl Acad Sci 110:7217–7222.

761 94. Lassalle F, Campillo T, Vial L, Baude J, Costechareyre D, Chapulliot D, Shams M,
762 Abrouk D, Lavire C, Oger-Desfeux C, Hommais F, Guéguen L, Daubin V, Muller D,
763 Nesme X. 2011. Genomic species are ecological species as revealed by comparative
764 genomics in Agrobacterium tumefaciens. Genome Biol Evol 3:762–781.

765 95. Geisselbrecht Y, Frühwirth S, Schroeder C, Pierik AJ, Klug G, Essen LO. 2012. CryB
766 from Rhodobacter sphaeroides: a unique class of cryptochromes with new cofactors.
767 EMBO Rep 13:223–229.

768 96. von Zadow A, Ignatz E, Pokorny R, Essen LO, Klug G. 2016. Rhodobacter sphaeroides
769 CryB is a bacterial cryptochrome with (6-4) photolyase activity. FEBS J 283:4291–4309.

97. Hördt A, López MG, Meier-Kolthoff JP, Schleuning M, Weinhold LM, Tindall BJ, Gronow S, Kyrpides NC, Woyke T, Göker M. 2020. Analysis of 1,000+ Type-Strain Genomes Substantially Improves Taxonomic Classification of Alphaproteobacteria. Front Microbiol 11:468.

98. Dikbas UM, Tardu M, Canturk A, Gul S, Ozcelik G, Baris I, Ozturk N, Kavakli IH. 2019. Identification and Characterization of a New Class of (6-4) Photolyase from Vibrio cholerae. Biochemistry 58:4352–4360.

99. Douki T, Cadet J. 2001. Individual determination of the yield of the main UV-induced dimeric pyrimidine photoproducts in DNA suggests a high mutagenicity of CC photolesions. Biochemistry 40:2495–2501.

100. Wu D, Lai W, Lyu C, Hang H, Wang H. 2018. UHPLC-Q-TOF/MS detection of UV-induced TpT dimeric lesions in genomic DNA. J Chromatogr 1096:135–142.

101. Banaś AK, Zgłobicki P, Kowalska E, Bażant A, Dziga D, Strzałka W. 2020. All You Need Is Light. Photorepair of UV-Induced Pyrimidine Dimers. Genes (Basel) 11:1304.

102. Kolmogorov M, Yuan J, Lin Y, Pevzner PA. 2019. Assembly of long, error-prone reads using repeat graphs. Nat Biotechnol 37:540–546.

103. Tatusova T, DiCuccio M, Badretdin A, Chetvernin V, Nawrocki E, Zaslavsky L, Lomsadze A, Pruitt K, Borodovsky M, Ostell J. 2016. NCBI prokaryotic genome annotation pipeline. Nucleic Acids Res 44:6614–6624.

104. Rodriguez-R LM, Konstantinidis KT. 2014. Bypassing Cultivation to Identify Bacterial Species Culture-independent genomic approaches identify credibly distinct clusters, avoid cultivation bias, and provide true insights into microbial species. Microbe Magazine 9:111–118.

105. Rodriguez-R LM, Konstantinidis KT. 2016. The enveomics collection: a toolbox for specialized analyses of microbial genomes and metagenomes. PeerJ Prepr 4:e1900v1.

106. Aziz RK, Bartels D, Best AA, DeJongh M, Disz T, Edwards RA, Formsma K, Gerdes S, Glass EM, Kubal M, Meyer F, Olsen GJ, Olson R, Osterman AL, Overbeek RA, McNeil LK, Paarmann D, Paczian T, Parrello B, Pusch GD, Reich C, Stevens R, Vassieva O, Vonstein V, Wilke A, Zagnitko O. 2008. The RAST Server: Rapid Annotations using Subsystems Technology. BMC Genomics 9:75.

107. Overbeek R, Olson R, Pusch GD, Olsen GJ, Davis JJ, Disz T, Edwards RA, Gerdes S, Parrello B, Shukla M, Vonstein V, Wattam AR, Xia F, Stevens R. 2014. The SEED and the Rapid Annotation of microbial genomes using Subsystems Technology (RAST). Nucleic Acids Res 42:D206.

108. Brettin T, Davis JJ, Disz T, Edwards RA, Gerdes S, Olsen GJ, Olson R, Overbeek R, Parrello B, Pusch GD, Shukla M, Thomason JA, III, Stevens R, Vonstein V, Wattam AR,

Xia F. 2015. RASTtk: A modular and extensible implementation of the RAST algorithm for building custom annotation pipelines and annotating batches of genomes. Sci Rep 5.

109. Madden T. 2002. The BLAST Sequence Analysis Tool. The NCBI Handbook 1–15.

110. Consortium TU, Bateman A, Martin M-J, Orchard S, Magrane M, Agivetova R, Ahmad S, Alpi E, Bowler-Barnett EH, Britto R, Bursteinas B, Bye-A-Jee H, Coetzee R, Cukura A, Da Silva A, Denny P, Dogan T, Ebenezer T, Fan J, Castro LG, Garmiri P, Georghiou G, Gonzales L, Hatton-Ellis E, Hussein A, Ignatchenko A, Insana G, Ishtiaq R, Jokinen P, Joshi V, Jyothi D, Lock A, Lopez R, Luciani A, Luo J, Lussi Y, MacDougall A, Madeira F, Mahmoudy M, Menchi M, Mishra A, Moulang K, Nightingale A, Oliveira CS, Pundir S, Qi G, Raj S, Rice D, Lopez MR, Saidi R, Sampson J, Sawford T, Speretta E, Turner E, Tyagi N, Vasudev P, Volynkin V, Warner K, Watkins X, Zaru R, Zellner H, Bridge A, Poux S, Redaschi N, Aimo L, Argoud-Puy G, Auchincloss A, Axelsen K, Bansal P, Baratin D, Blatter M-C, Bolleman J, Boutet E, Breuza L, Casals-Casas C, de Castro E, Echioukh KC, Coudert E, Cuche B, Doche M, Dornevil D, Estreicher A, Famiglietti ML, Feuermann M, Gasteiger E, Gehant S, Gerritsen V, Gos A, Gruaz-Gumowski N, Hinz U, Hulo C, Hyka-Nouspikel N, Jungo F, Keller G, Kerhornou A, Lara V, Le Mercier P, Lieberherr D, Lombardot T, Martin X, Masson P, Morgat A, Neto TB, Paesano S, Pedruzzi I, Pilbout S, Pourcel L, Pozzato M, Pruess M, Rivoire C, Sigrist C, Sonesson K, Stutz A, Sundaram S, Tognolli M, Verbregue L, Wu CH, Arighi CN, Arminski L, Chen C, Chen Y, Garavelli JS, Huang H, Laiho K, McGarvey P, Natale DA, Ross K, Vinayaka CR, Wang Q, Wang Y, Yeh L-S, Zhang J, Ruch P, Teodoro D. 2021. UniProt: the universal protein knowledgebase in 2021. Nucleic Acids Res 49:D480–D489.

111. Pearson WR. 2013. An Introduction to Sequence Similarity ("Homology") Searching. Curr Protoc Bioinformatics 42:3.1.1-3.1.8.

112. Alikhan NF, Petty NK, Ben Zakour NL, Beatson SA. 2011. BLAST Ring Image Generator (BRIG): Simple prokaryote genome comparisons. BMC Genomics 12:1–10.

113. Krueger F. 2021. TrimGalore: A wrapper around Cutadapt and FastQC to consistently apply adapter and quality trimming to FastQ files, with extra functionality for RRBS data. GitHub.

114. Götz S, García-Gómez JM, Terol J, Williams TD, Nagaraj SH, Nueda MJ, Robles M, Talón M, Dopazo J, Conesa A. 2008. High-throughput functional annotation and data mining with the Blast2GO suite. Nucleic Acids Res 36:3420–3435.

841 **Fig. 1. Comparison of phylogenetic relatedness among the bacterial strains and their**
842 **tolerance to UVCR. (A)** Maximum-likelihood analysis of 16S rRNA gene sequences from the
843 stratospheric isolates and closely related strains. UVCR tolerance of the **(B)** actinobacterial and
844 **(C)** betaproteobacterial strains based on the surviving number of cells (N) at each UVCR dose
845 divided by that in unexposed populations (N_0). The values plotted are averages from three
846 independent replicates. Error bars represent SEM.
847
848 **Fig. 2. DNA repair and ROS detoxification genes in *Curtobacterium* sp. L6-1 not found in**
849 **strain DSM 20129.** Genomes were compared using the BLAST Ring Image Generator (BRIG)
850 with the blastp algorithm. Rings represent the following (from innermost to outermost): **1)** GC
851 Content, **2)** GC skew of the L6-1 genome, **3)** percent identity to L6-1 of protein orthologs found
852 in strain DSM 20129, and **4)** DNA repair (**black**) and ROS detoxification (grey) genes. Genes
853 present in L6-1 but absent in DSM 20129 are indicated in red text.
854
855 **Fig. 3. DNA repair and ROS detoxification genes in *Noviherbaspirillum* sp. L7-7A not found**
856 **in strains TSA40 and TSA66.** Genomes were compared using the BLAST Ring Image Generator
857 (BRIG) with the blastp algorithm. Rings represent the following (from innermost to outermost):
858 **1)** GC Content, **2)** GC skew of the L7-7A genome, **3)** percent identity to L7-7A of protein
859 homologs found in strains TSA40 and TSA66, and **4)** DNA repair (**black**) and ROS detoxification
860 (grey) genes. Genes present in L7-7A but absent in both TSA40 and TSA66 are indicated in red
861 text.
862
863

Fig. 4. Directed evolution of UVCR tolerance in strain DSM 20129. A) Schematic depiction of the directed evolution method used to improve UVCR tolerance in strain DSM 20129. The details of the procedure are descried in the text. **B)** UVCR tolerance of DSM 20129 after each round of UVCR exposure as compared to isolate L6-1, measured as the number of surviving CFUs (N) at each UVCR dose divided by total number of CFUs in the unexposed control (N_0). Data shown are the average of three independent replicates. Error bars represent SEM. **C)** Summary of the mutations acquired during the directed evolution process. Mutation type (smaller pie chart) refers only to the mutations occurring in coding sequences (green slice in larger pie chart). Gene Ontology (GO) function annotations were determined for proteins that acquired amino acid point mutations in their coding sequence (blue slice in smaller pie chart).

Fig. 5. Cellular ROS concentrations and photolyase activity determination in UVCR treated cells. A) Intracellular ROS concentrations were quantified in the stratospheric isolate (L6-1), the DSM 20129 wild-type parent (DSM 20129), and UV-evolved strain (DSM-9.3.3) using the free radical probe H_2DCFDA. *E. coli* MG1655 and *D. radiodurans* R1 were used as controls and for comparison. The average of three independent replicates with error bars representing SEM are plotted. **B)** UVCR survival of strains under dark repair and photoreactivating (light) conditions. Inset: Percent increase in LD_{90} after 1 h incubation in white light vs. dark after UVCR exposure. The data plotted are averages of four independent replicates with error bars representing SEM. (ns = not significant; ** = P-value < 0.01; *** = P-value < 0.001; one-way ANOVA and Tukey's post-test).

Table 1: General genome features of the stratospheric isolates and closely related reference strains.

Strain	Chr	Plasmids	Size (Mbp)	GC %	Genes	rRNA	tRNA	Proteins	ANI (±SD) %	AAI (±SD) %
Curtobacterium sp. L6-1	1	0	3.4	72.0	3,158	12	46	3,072	83.64 ± 4.97	79.97 ± 13.57
Curtobacterium flaccumfaciens DSM 20129	1	1	3.8	70.9	3,616	9	47	3,517		
Noviherbaspirillum denitrificans TSA40	n.d.	n.d.	5.8	61.5	5,771	6	51	5,446	79.43 ± 4.89	65.93 ± 18.08
Noviherbaspirillum sp. L7-7A	3	0	5.2	62.0	4,771	15	64	4,581	79.24 ± 4.83	67.38 ± 17.84
Noviherbaspirillum autotrophicum TSA66	n.d.	n.d.	5.4	59.9	5,130	15	59	4,980		

887

Table 2: Mutations acquired in strain DSM 20129 during the directed evolution process.

Location	Position	Mutation	Strain of 1st Occurrence						Annotation	Gene/Locus Tag	Description
			WT	1	3	6	7	9			
Chr	7,692	G→C		X					D180H (GAC→CAC)	K0028_00025 →	NAD(P)/FAD-dependent oxidoreductase
Chr	72,765	T→C				X			F122L (TTC→CTC)	trmD →	tRNA (guanosine(37)-N1)-methyltransferase TrmD
Chr	160,708	C→A					X		P183T (CCG→ACG)	K0028_00715 →	uracil-DNA glycosylase
Chr	205,567	G→A					X		E84K (GAG→AAG)	prfA →	peptide chain release factor 1
Chr	217,440	C→T						X	H457Y (CAC→TAC)	atpD →	F0F1 ATP synthase subunit beta
Chr	559,194	C→G				X			Q15H (CAG→CAC)	K0028_02565 ←	flagellar hook capping protein
Chr	612,632	C→A						X	A37S (GCC→TCC)	K0028_02820 ←	RNA polymerase sigma factor
Chr	682,540	C→G				X			A171P (GCC→CCC)	K0028_03160 ←	GrpB family protein
Chr	1,015,248	T→C				X			K13R (AAG→AGG)	K0028_04710 ←	cold-shock protein
Chr	1,073,811	G→A					X		G170S (GGC→AGC)	K0028_05010 →	carbohydrate-binding protein
Chr	1,173,658	G→T		X					R410L (CGG→CTG)	K0028_05480 →	HAMP domain-containing histidine kinase
Chr	1,448,846	G→C						X	A343G (GCG→GGG)	K0028_06725 ←	transaldolase family protein
Chr	1,750,735	2 bp→CT				X			coding (162-163/1803 nt)	K0028_08150 ←	S8 family serine peptidase
Chr	2,439,407	G→A				X			D78N (GAC→AAC)	K0028_11565 →	L-serine ammonia-lyase
Chr	2,583,948	C→A						X	V95F (GTC→TTC)	coaA ←	type I pantothenate kinase
Chr	2,778,691	A→G		X					L78P (CTG→CCG)	K0028_13275 ←	phosphotransferase
Chr	3,362,910	A→G						X	W367R (TGG→CGG)	K0028_16065 ←	DNA photolyase family protein
Chr	3,363,495	G→T						X	P172T (CCC→ACC)	K0028_16065 ←	DNA photolyase family protein
Plasmid	42,326	T→G						X	V108G (GTG→GGG)	K0028_17640 →	inorganic diphosphatase
Plasmid	63,755	G→A		X					W396* (TGG→TGA)	metK →	methionine adenosyltransferase

888

889

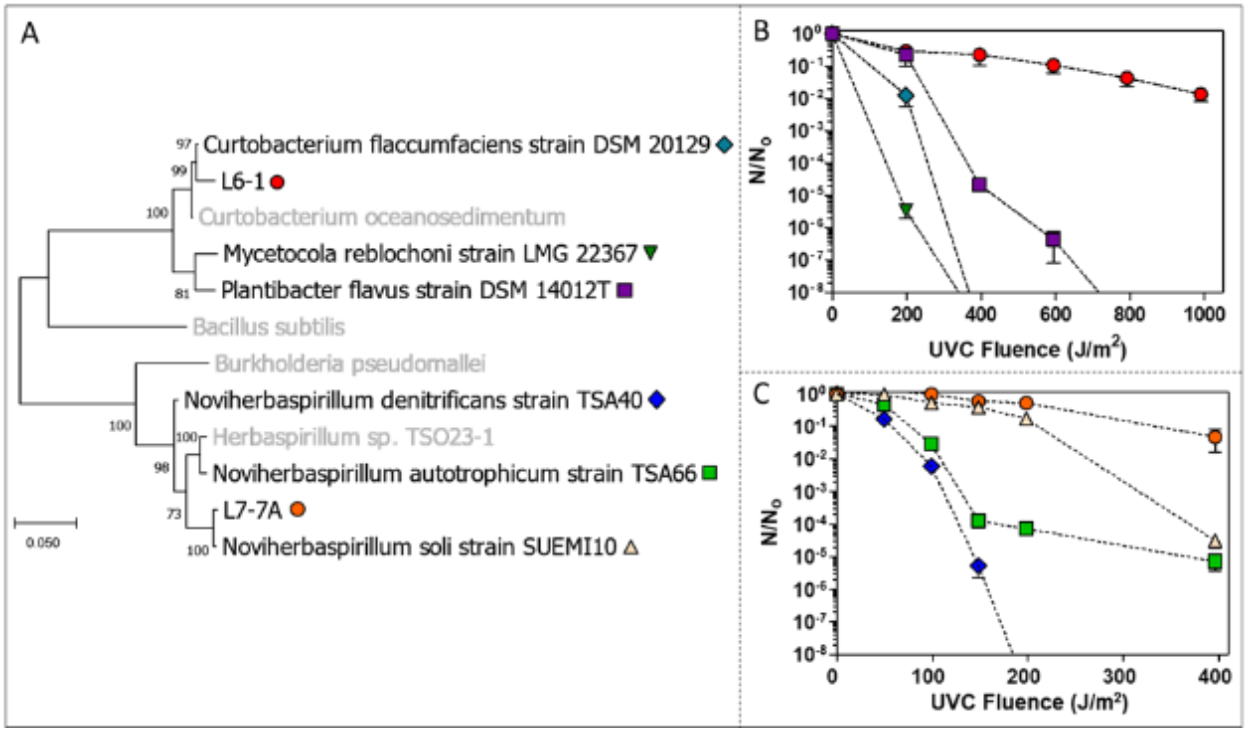

890

891

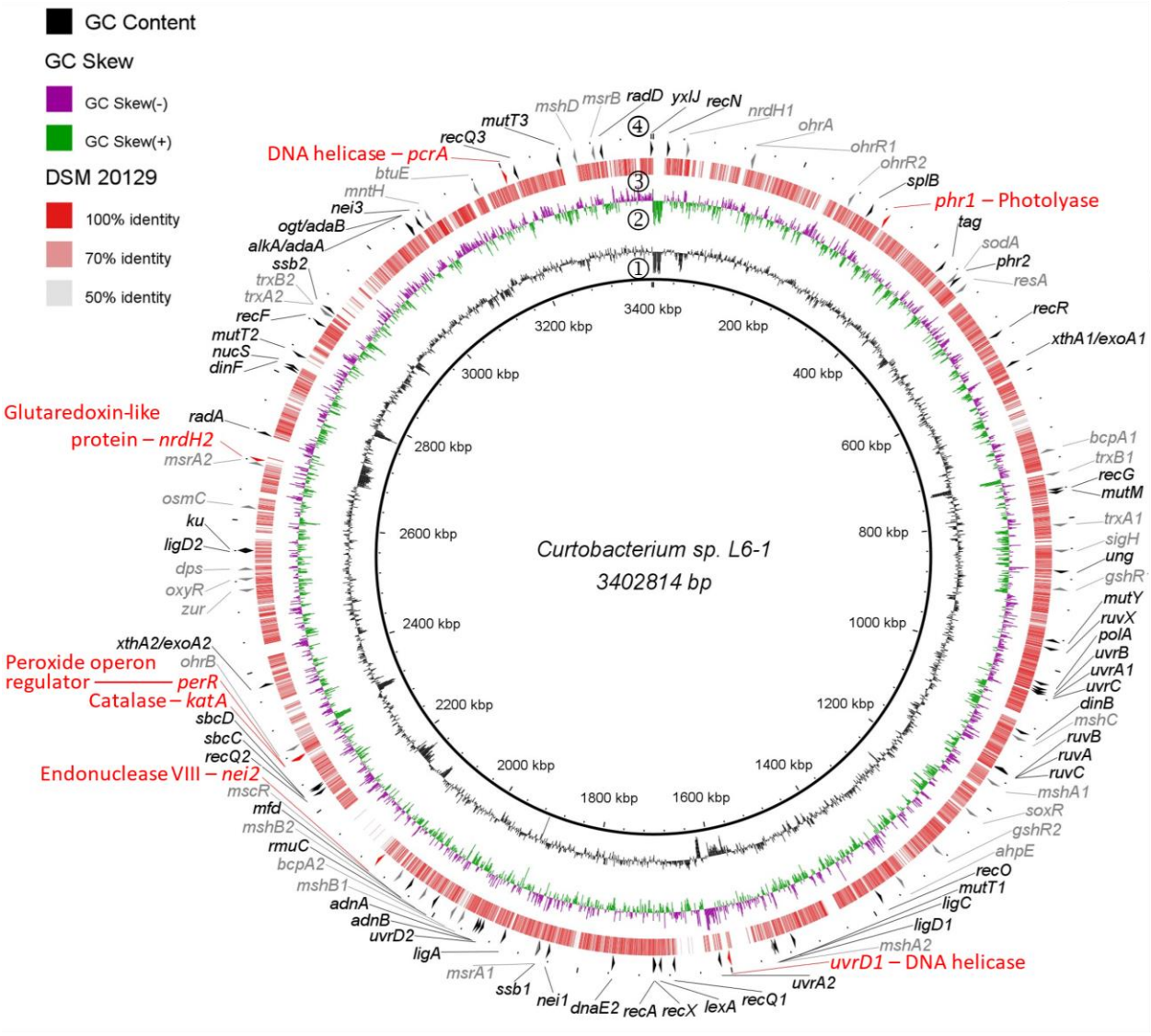

892

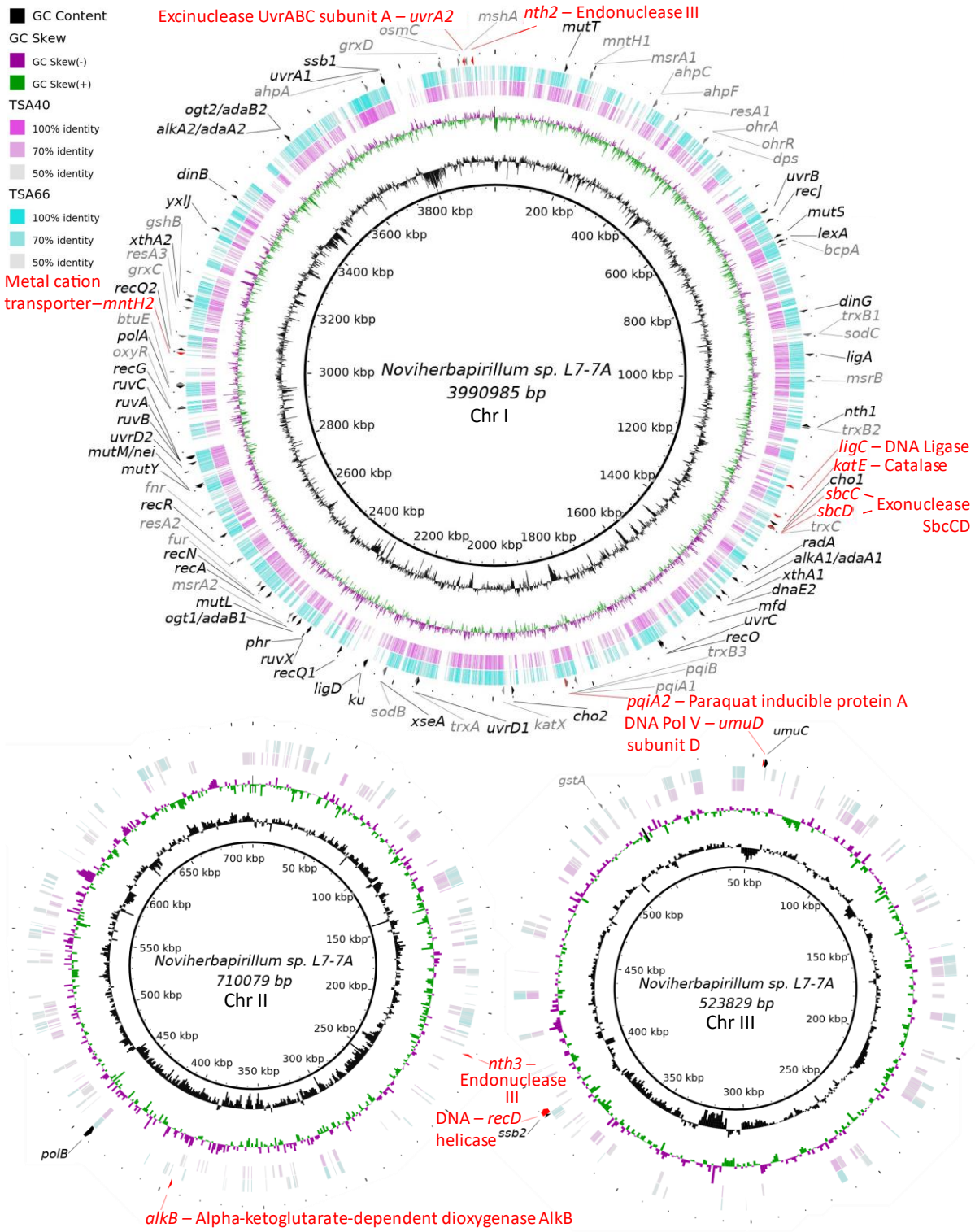

893

894

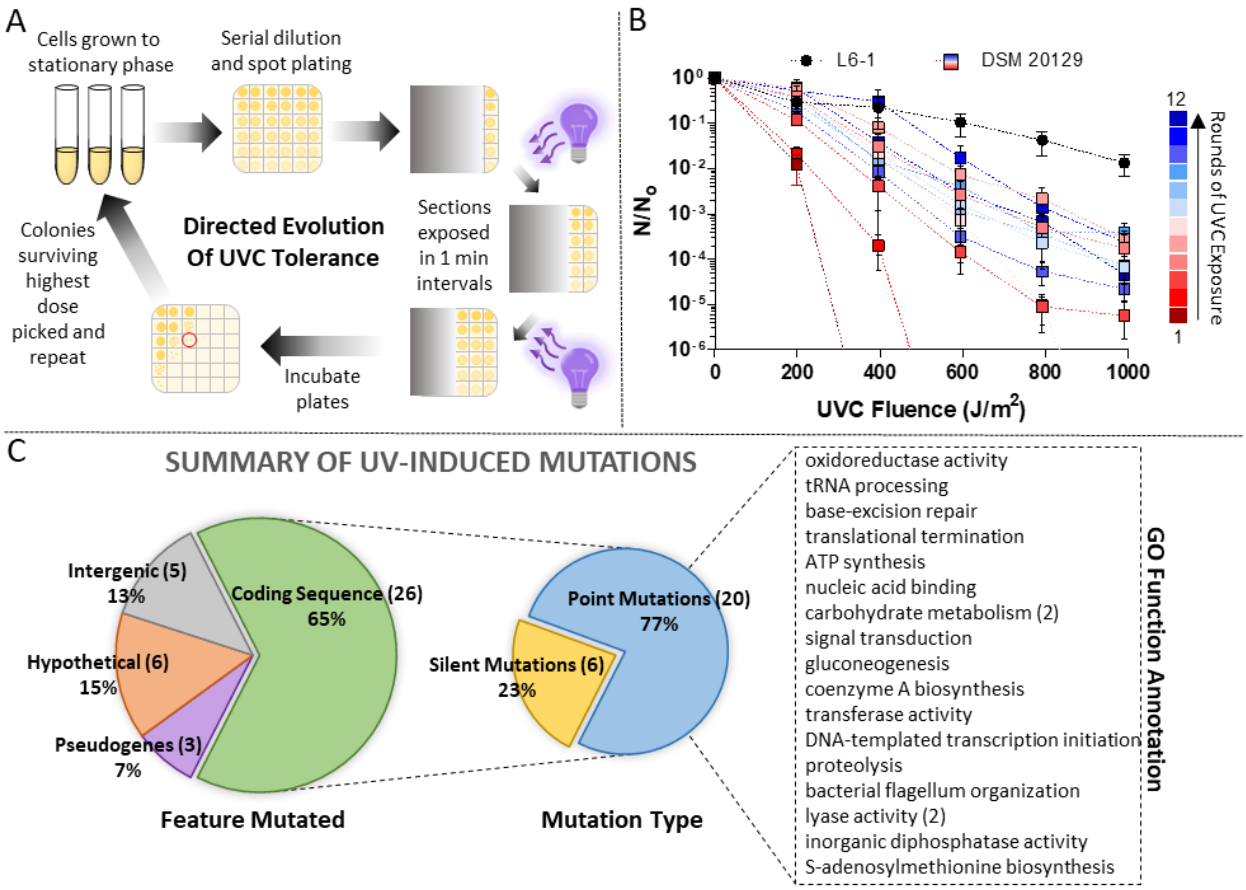

895

896

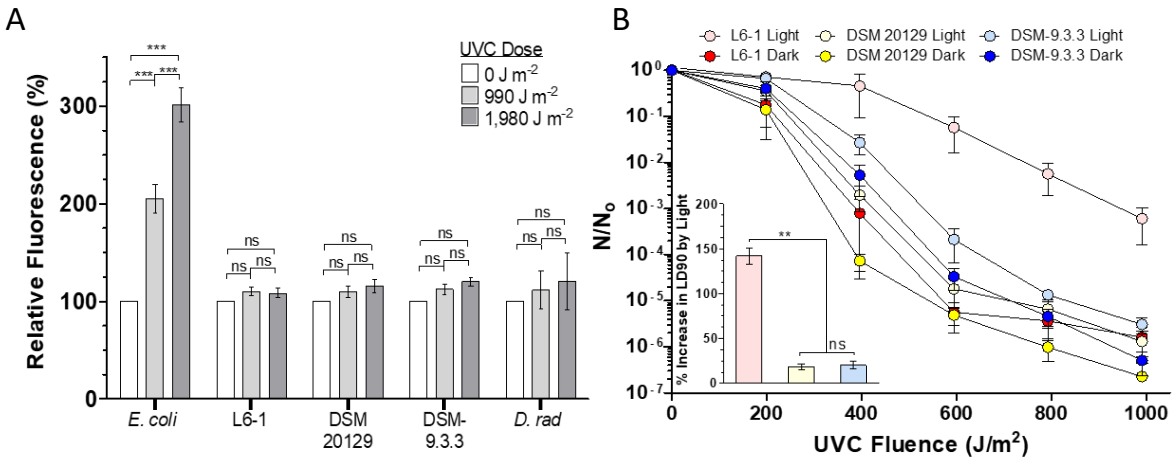

897